69th International Astronautical Congress (IAC), Bremen, Germany, 1-5 October 2018.

IAC-18,A7,3,1,x44363

Solar Wind Analyzer – The Solar Orbiter milestone towards on-board intelligent decision making systems

L. Amoruso[a]*, C.J. Owen[b] , V. Fortunato[a], R. De Marco[c], R. Bruno[c], M. Salatti[d]

[a] *Planetek Italia S.r.l., Via Massaua 12, I-70132 Bari, Italy, 0809644200,* amoruso@planetek.it
[b] *University College London, Mullard Space Science Laboratory, Department of Space & Climate Physics, Holmbury St. Mary, Dorking, United Kingdom, RH5 6NT,* c.owen@ucl.ac.uk
[c] *National Institute for Astrophysics, Institute for Space Astrophysics and Planetology, Via del Fosso del Cavaliere 100, Rome, Italy, 00133,* roberto.bruno@iaps.inaf.it
[d] *Italian Space Agency, Via del Politecnico snc, Rome, Italy, 00133,* mario.salatti@asi.it

* Corresponding Author

Abstract

The most important challenge underpinning the transition to next generation of space missions design is the discrepancy between the dramatic increases in observation rate and the marginal increase in downlink capacity, enforcing the shift from the traditional "acquire-compress-transmit" paradigm to highly efficient intelligent on-board processing of observations, minimizing downlink requirements while respecting the limitations in power and bandwidth resources. Solar Orbiter (SO), an ESA/NASA mission, is a milestone both in the purely technological and scientific sphere.

SO is designed to study the connection between the Sun and the heliosphere, with particular interest to open issues such as the sources of solar wind streams and turbulence, the heliospheric variability, the origin of energetic particles and the solar dynamo. The selected science payload is required to support making the link between in-situ and remote sensing observations, and is composed of ten instruments or suites of instruments including spectrometers, imagers, wave and particle instruments – many the result of large international consortia. In particular, the plasma suite Solar Wind Analyzer (SWA) comprises: Proton-Alpha Sensor (PAS), Electron Analyzer System (EAS), Heavy Ion Sensor (HIS) together with the Data Processing Unit (DPU), and will provide high-resolution 3D velocity distribution function of ions and electrons, together with ion composition, necessary to infer the thermal state of solar wind and its source regions, identify structures such as shocks, CME's and other transients, and determine the link between particle dynamics and waves. SO will explore new distance and latitude regions that remain unexplored, even accounting for existing Helios and upcoming Parker Solar Probe observations.

The technical challenges include heavy constraints such as the limited bandwidth available to SWA for downlink, so that the whole set of raw particle data collected cannot be transmitted back to ground. Data processing is thus used to evaluate concise scientific properties of the solar wind, particularly the moments of the particle velocity distribution functions (VDF), such that it is then acceptable to transmit the full VDF data only at low frequencies. Then processing is re-adopted on these distributions to meet the required (lossless) compression rates (2-8).

Another step towards the aforementioned paradigm shift is represented by the SWA Book-Keeping Algorithm (BKA), which has been designed to ensure that the individual sensors remain within the allocated telemetry rate on an orbit-averaged basis. The philosophy of the SWA book-keeping scheme has since been applied to all instruments with ESOC's Operations Team introducing the concept of Operations Telemetry Corridors (OTC) to finely tune the rate of telemetry generation by the instruments.
Keywords: (on-board, operations, autonomy)

Acronyms/Abbreviations

European Space Agency (ESA), National Aeronautics and Space Administration (NASA), Consultative Committee for Space Data Systems (CCSDS), Astronomical Unit (AU), Solar Orbiter (SO), Solar Wind Analyzer (SWA), Electron Analyzer System (EAS), Proton-Alpha Sensor (PAS), Heavy Ion Sensor (HIS), Velocity Distribution Function (VDF), Book-Keeping Algorithm (BKA), Operations Telemetry Corridors (OTC), Data Processing Unit (DPU), Housekeeping (HK), Normal Mode (NM), Burst Mode (BM), static Random Access Memory (SRAM), Solid State Mass Memory (SSMM),

1. Introduction

Solar Orbiter is ESA's first M-Class mission under the Cosmic Vision 2015-2025 Program. It is funded by ESA, NASA and many European National Agencies; currently the schedule is dictated by a baseline launch date in February 2020. After the cruise phase and multiple gravity-assist manoeuvres (Venus, Earth) the spacecraft will operate on an elliptical orbit bringing it to a minimum perihelion distance of ~60 solar radii (0.28 AU), where it will make unprecedented measurements. Furthermore, another unique feature, which distinguishes SO from other previous and current missions, is the raising of the inclination to high latitudes (in excess of 30° by end of mission), which allows an unprecedented view of the poles of the Sun. All these aspects contribute significantly to the final goal of the mission, which is to establish the fundamental physical links between the highly dynamic magnetized atmosphere of the Sun and the solar wind in all its quiet and disturbed states.

The scientific payload of the SO mission is composed of ten experiments. Among the instruments, the Solar Wind Analyser suite, with its four sensors, will provide at high time resolution the velocity distributions for protons, alphas particles and electrons, together with measurement of minor heavy ions.

The Data Processing Unit performs all the suite management tasks, together with scientific data processing (related to protons and electrons fluxes) in order to compress the science data stream by adapting the collected data rate to the limited telemetry bandwidth allocated to the suite. Due to SO unique mission and orbit features, the required compression rates range from 2 to 8, according to the different kinds of measured data and associated data product' volumes.

Thus, highlighting the need of a coordinate set of techniques shared between the DPU and the Ground Segment to ensure the maximization of the science return without prejudice to allocated downlink limits.

Such challenges, like onboard autonomous decision-making systems and operations, are nowadays pervasive in the whole space value chain: from the user-service interaction to satellite platform, from service performances to ground segments, from resources management to mission planning.

The SO Ground Operations procedures and the specific SWA telemetry management mechanism, represent a milestone use case towards such paradigm shift.

1.1 Solar Wind Analyser instrument suite

The SWA suite [1]-[2] composes of four sensors and the DPU. Sensors are

- the Electron Analyser System, with its two heads, intended to make the high resolution determination of the core, halo and strahl electron velocity distribution functions (VDFs) in the solar wind (energy ranging from 1 eV to 5 KeV) and their moments
- the Proton & Alpha Sensor, sampling the VDFs of proton and alpha particles (energy ranging from 0.2 to 20 KeV/q) at high time resolution equivalent to the ambient proton cyclotron period
- the Heavy Ions Sensor, measuring major charge states of C, O and Fe, 3D VDFs of prominent heavy solar wind ions, suprathermal ions and pick-up ions of various origins, such as weakly ionized species (He+, O+).

Each sensor has been designed to operate near-continuously, collecting (i.e. count) different particles carried by the solar wind, sampling all or part of the full sky with a scan of azimuth angles, elevation angles and energy levels. Such measures, produce a variety of data products in different operational modes: the Normal Mode (NM), expected to cover more than the 99% of sensors duty cycles, and Burst Mode (BM) is used in the remaining 1% actually less than. In addition, the DPU is able to support the provision of high-resolution data through a Triggered mode, which will be enacted in response to a trigger signal generated externally, via the S/C, or by one of the other in-situ instruments.

Considering this operational environment, the DPU's data processing strategy is twofold: the nominal bandwidth allocated to SWA, details in Table 1, is limited to a 14.5 KiB/s average rate, thus a double data reduction approach has been adopted.

A regular (continuous) wind flux characterization via moments computation, producing a statistical characterization of the wind (considered as a plasma flux) with synthetic parameters, and a full raw data transmission at longer intervals, compressed if necessary.

Table 1. SWA Telemetry Allocations

Sensor	Telemetry allocation [bps]	SSMM load (Gbits per 168 day orbit)
SWA/EAS	4345.4	63.1
SWA/HIS	5512.5	80.0
SWA/PAS	4455.4	64.7
SWA/DPU + HK	300	4.35
Total	14613.3	212.1
Project Allocation	14500	210.5

In addition to this, it is anticipated that there will be periods of significant length during the cruise phase, in which SWA may be required to operate at < 25 % of its nominal telemetry rate.

The only way to meet these requirements and such level of flexibility is to define a process intelligent enough to disable, in autonomy, all the most data demanding modes of operations and by reducing the time cadence of the normal mode data products to a level compatible with the available telemetry resource.

2. Scientific data modeling perspective

Most of our knowledge about solar wind, in the inner heliosphere, derives from observations from the late 70's performed by Helios 1 & 2, [3]-[4]-[5]. Meanwhile more recently, late 90's / early 2000, new insights into the magnetosphere and the solar wind have been a key output of the ESA\Cluster mission [6]-[7]-[8] that has been used to probe the detail of the wind, the NASA-WIND s/c [9], launched in 1994 and put at the Lagrange point L1 on 2004 to monitor the solar wind and the NASA-ACE (Advanced Composition Explorer) [10] launched in 1997 and mainly dedicated to study the solar wind minor ions composition.

Starting from this practical knowledge of the solar wind constituents and considering the aforementioned telemetry downlink constraints, a two-step approach has been adopted in order ensure all the mission objectives allocated to SWA [1].

As a first step, since the moments of the plasma VDFs and their spatial gradients play a key role in the quantitative description of plasma behaviour, a custom implementation dedicated to all solar wind particles populations has been designed and engineered to operate at higher cadence. This requires an extreme level of compression to be coupled with specific lossless compression algorithms to be applied to full counts distributions. Subsections 2.1 details all these approaches.

In parallel, as discussed in Section 3, a mechanism has been designed, by Owen et al [21], enabling the DPU to be capable of imposing data collection and/or mode use and/or telemetry generation restrictions on each of the three SWA sensors separately in order to keep each of them within their respective allocations.

2.1 Information Theory approach

A compression process is ideally based on the principle of removing unnecessary redundancy in data, while preserving their information content (entirely or partially for lossless and lossy methods respectively). In fact, any non-random data has some structure, and this structure can be exploited to achieve a smaller representation of the data itself: the smallest one is a representation where no structure is discernible. Goal of compression is to minimize the data representation, so to save transmission band.

Redundancy is thus a key concept in data compression. Nevertheless, data structure is not the only thing can be exploited to obtain compression: another key concept is irrelevance, based on the user needs, which forms the basis of any lossy compression approach.

An important logical scheme to keep in mind when addressing any data compression issue, consists of two development stages:

1. The first phase is usually referred to as *modeling*. In this phase data are modelled in order to characterize their redundancy. The difference between the data and the model is referred as residual
2. The second phase is called *coding*. A description of the model and how data differ from the model.

The model identified in data (the type of structure they have) defines as well their redundancy. Data are distributed according to a certain law; it is a fundamental assumption in compression tasks (fully random data almost cannot be compressed) Once this law is identified, it is used in order to predict the value of each element in the sequence: so the information to be kept, and then encoded, are no more data values, but only the difference between them and their prediction, i.e. the so-called residuals. In a lossy compression approach residuals are then heavily reduced according to the part of information having no (or less) interest within the application domain; so discarding part of data information content turns into the benefit of a higher compression ratio.

Coding is the assignment of a binary sequence to each element of an alphabet (i.e. a set of data values); sequences are defined in order to reduce the number of bits required to represent different messages (combinations of the alphabet's elements). A different number of bits can be assigned in representing different symbols. Assigning shorter sequences to represent symbols occurring more often allows to reach a lower average bit rate per symbol. This is the key point in variable-length codes (e.g. Huffman codes). Obviously coding scheme has to ensure de-codability: so any given sequence of codewords has to be univocally decoded.

A quantitative measure of the data information content has to be introduced. Assuming that x is a discrete random variable that takes values in a finite alphabet X, being $P(x)$ the probability of a single symbol x, the entropy (to be more precise, the first-order entropy) of X is defined by:

$$H(X) := \sum_{x \in \chi} p(x) \log_2 \frac{1}{p(x)} \tag{1}$$

Where the unit of information depends on the base of the log2.

Entropy is a measure of the initial uncertainty or equivalently of the generated information. In general, it is not possible to know the entropy for a source (of information), but the statistical model of the physical phenomenon can be used as its best approximation. The better compression performance is achieved, as the model is closer to match the information source. Entropy assumes a particular relevance considering that its value is, for a given source, the minimum number of bits needed to fully represent any possible data the source could generate, without exploiting additional characterizations. Thus, when adopting an entropy coder alone (with no per-processing step) the minimum number of bits needed to represent data is equal to the entropy.

Starting from this approach and because of measurement principles designed for both EAS and PAS instruments, it is clear that all the data products might be modelled as information sources producing symbols highly correlated in both time and spatial dimension.

In fact, as discussed in [12], a single particle in plasma can be completely described by its mass, its charge and its position in Cartesian space and velocity space at a given time. Let us consider a volume unit *dV*, small but finite, containing a number of particles equal to *NdV*, where *N* represents the number density.

Each particle has its own velocity; thus, the *NdV* particles can be represented also in the velocity space. In the Cartesian space, particle number density is $N(x,y,z,t)$, and in the velocity space density is called *velocity distribution function* and is defined as $f(v_x,v_y,v_z,x,y,z,t)$.

The model applied to this distribution function and the subsequent experimental evidences due to an extensive trade-off phase between computational needs and onboard computational resources, led to the implementation of the following double data compression strategy.

2.1.1 SWA Moments calculation

Given the distribution function *f*, one can define the *n*-th order moment, in the satellite reference frame as [11]:

$$M_n = \int f(\mathbf{v})\mathbf{v}^n d\mathbf{v} \quad (2)$$

The moment of order zero is called number density and it is defined as:

$$n = \int f(\mathbf{v}) d\mathbf{v} \quad (3)$$

The first order moment is called number flux density vector:

$$n\mathbf{V} = \int \mathbf{v} f(\mathbf{v}) d\mathbf{v} \quad (4)$$

From which one can compute the flux velocity by dividing for n.

The second order moment is the momentum flux density tensor:

$$\boldsymbol{\Pi} = m \int \mathbf{v}\mathbf{v} f(\mathbf{v}) d\mathbf{v} \quad (5)$$

Finally, the third order moment is the energy flux density vector:

$$\mathbf{Q} = \frac{m}{2} \int v^2 \mathbf{v} f(\mathbf{v}) d\mathbf{v} \quad (6)$$

It is also possible to compute higher order moments but they do not have a physical meaning.

The last two equations can be written in the form:

$$\mathbf{P} = \boldsymbol{\Pi} - \rho\mathbf{V}\mathbf{V}$$
$$\mathbf{H} = \mathbf{Q} - \frac{1}{2}Tr(\mathbf{P})\mathbf{V} - \mathbf{V} \cdot \mathbf{P} - \frac{1}{2}\rho V^2 \mathbf{V} \quad (7)$$

being $\mathbf{V}$ the ratio between the first-order moment and the zero-order moment and, $\rho = mn$ the density expressed as the zero-order moment times the mass of the particle under analysis.

Furthermore, moment flux density tensor and the heat flux density vector can be projected in the plasma reference frame:

$$\mathbf{P} = m \int (\mathbf{v} - \mathbf{V})(\mathbf{v} - \mathbf{V}) f(\mathbf{v}) d\mathbf{v}$$
$$\mathbf{H} = \frac{m}{2} \int (\mathbf{v} - \mathbf{V})^2 (\mathbf{v} - \mathbf{V}) f(\mathbf{v}) d\mathbf{v} \quad (8)$$

Obtaining the pressure tensor P and the heat flux vector H respectively.

All the moments presented in the previous section, can be written by means of the particle count rate measured by one of the SWA instruments. As a matter of fact both EAS and PAS measure the number of particle having a given energy level e, a given azimuth angle φ, and an elevation angle θ.

Let us consider a particle flux coming from a particular direction (θ,φ):

$$F = \iiint v f d\mathbf{v} \quad (9)$$

Flux incident to the instrument is not entirely transmitted because the instrument has an effective cross-section S. Thus, the number of particles registered by the instrument is:

$$C = \iiint S v f d\mathbf{v} \quad (10)$$

Switching to discrete quantities, one can write $d\mathbf{v}$ as:

$$\Delta\mathbf{v} = v_i^2 \Delta v_i \cos\theta_j \Delta\varphi_k \Delta\theta_j \quad (11)$$

Where Δv_i is the amplitude of the energy channel, $\Delta\theta_j$ and $\Delta\varphi_k$ are the amplitude of the elevation and azimuth angle sector.

The distribution function formula can be written as:

$$f = \frac{C_{i,j,k}}{v_i^4 G T} \quad (12)$$

expressed in physical units $\left[\frac{m^4}{s^4}\frac{sr\,m^2 eV}{eV}\,s\right]^{-1} = 1/(m^6 sr/s^3)$.

Two quantities have been introduced here:

- the geometrical factor $|G| = (sr \cdot m^2 eV)/eV$
- and the accumulation time T=(NENERGY *NPOLAR)$^{-1}$, being NENERGY, NPOLAR the number of energy levels and polar angles respectively, e.g. assuming value {64, 16} for EAS and {96, 9} for PAS.

Hence, given:

$$f\Delta v = \frac{C_{i,j,k}}{v_i^4 G T} v_i^2 \cos\theta_j \,\Delta v_i \Delta\theta_j \Delta\varphi_k = dn_{i,j,k} \quad (13)$$

one can perform moments calculation as follows:

$$n = \sum_{i,j,k} dn_{i,j,k} \quad (14)$$

$$nV_x = \sum_{i,j,k} v_i \cos\theta_j \cos\varphi_k \, dn_{i,j,k} \quad (15)$$

$$nV_y = \sum_{i,j,k} v_i \cos\theta_j \sin\varphi_k \, dn_{i,j,k} \quad (16)$$

$$nV_z = \sum_{i,j,k} v_i \sin\varphi_k \, dn_{i,j,k} \quad (17)$$

$$\Pi_{xx} = m\sum_{i,j,k} (v_i \cos\theta_j \cos\varphi_k)^2 dn_{i,j,k} \quad (18)$$

$$\Pi_{xy} = m\sum_{i,j,k} (v_i \cos\theta_j \cos\varphi_k)(v_i \cos\theta_j \sin\varphi_k) dn_{i,j,k} \quad (19)$$

$$\Pi_{xy} = m\sum_{i,j,k} (v_i \cos\theta_j \cos\varphi_k)(v_i \cos\theta_j \sin\varphi_k) dn_{i,j,k} \quad (20)$$

$$\Pi_{yy} = m\sum_{i,j,k} (v_i \cos\theta_j \sin\varphi_k)^2 dn_{i,j,k} \quad (21)$$

$$\Pi_{yz} = m\sum_{i,j,k} (v_i \cos\theta_j \sin\varphi_k)(v_i \sin\theta_j) dn_{i,j,k} \quad (22)$$

$$\Pi_{zz} = m\sum_{i,j,k} (v_i \sin\theta_j)(v_i \sin\theta_j) dn_{i,j,k} \quad (23)$$

$$Q_x = \frac{m}{2}\sum_{i,j,k} v_i^2 (v_i \cos\theta_j \cos\varphi_k) dn_{i,j,k} \quad (24)$$

$$Q_y = \frac{m}{2}\sum_{i,j,k} v_i^2 (v_i \cos\theta_j \sin\varphi_k) dn_{i,j,k} \quad (25)$$

$$Q_z = \frac{m}{2}\sum_{i,j,k} v_i^2 (v_i \sin\theta_j) dn_{i,j,k} \quad (26)$$

From an operational point of view, all the equations above have been conducted thus obtaining a series of Look-Up Tables (LUT) allowing to perform moments calculation by means of only sums and products, actually having a count "modulated" by a combination of these factors.

In fact, one can consider that a generic moment of $O\text{-}th$ order for the Solar Wind can be computed as summation of products

$$M(O^{th}) = \sum_i \sum_j \sum_k M_{O_{ijk}} dn_{ijk} \quad (27)$$

being i index accounts for the energy bins, j for the azimuth and k for the elevation intervals.

These constant matrices $M_{O_{ijk}}$, each one composed, as an example, of 32x16x64 (= 32768) elements for each of the two EAS sensors heads and 96x9x11(= 9504) for PAS, can be computed once, stored in static Random Access Memory (SRAM) as LUTs and properly used on-the-fly while accumulating moments for a given measured distribution.

Even though this choice allows moments computation to be considerably simplified at run-time, ultimately considering the sampled Solar Wind particles counts (16 bit integer values) as the only critical "source of variability", their storage requires approximately 3.5 Mbytes of SRAM, unsustainable due to 25% required margin to be applied on DPU's 8 Mbyte memory, thus leaving to scientific processing about just 4 Mbyte for all its processing tasks. Although the algorithm flow has not been modified in its architecture, the optimal compromise between processing limitations in terms of both memory and computing time relies on the need for a specific data layout: thus, we introduced the concepts of Pixels and Layers to represent the information coming from both EAS and PAS sensors.

Pixels

We define a pixel as a point in [azimuth, elevation] space, which is observed by a sensor. Each sensor provides a *WxH* 2D array of pixels (an image) for each energy level. This allows tuning algorithms to work on 32x16 pixels (EAS) and 11x9 pixels (PAS) images in the worst case.

Layers

A layer is a 2D array of pixels. Given the definition of a pixel, EAS and PAS data are received and distributed into a working structure based on a set of layers of *WxH* pixels each. One layer for each energy level is defined so that EAS data are formed by 64 layers and PAS data are formed by 96 layers. Processing is then performed on each WxH image. The core-processing unit of an image is then used as a way to dynamically distribute computation load on more activities as required by Flight Application Software.

The concept of "Layer" allows optimizing LEON2 cache memory utilization [19], given locality of most frequently used data. Since moments computation formulas depend on specific constants that are computed at initialization time, these constant values are stored directly into layers, whenever the constant values depend "only" on energy level. On the other side, constants depending only on azimuth and elevation are stored into specific control structures.

Such level of decomposition on the intrinsic nature of the data, we recall started from the equations (2) and (9), have been exploited to define the best-implementable algorithm for lossless compression to be applied to VDFs, contextually able to meet both real-time processing requirements and the aforementioned downlink requirements.

2.1.2 SWA Lossless data compression

The goal of this trade-off analysis is to assess processing performances, from both data compression ratios and its computational load points of view, considering that processing time is a limited resource, as is the telemetry volume.

Analyses have been conducted over a number of steps: first of all the worst case for compression was identified considering all the data products, their volumes and their generation rates. Each of the EAS sensors produces 32768 samples (@ 16 bit/sample), resulting in 512 Kbps which, in one of the modes, have to be compressed in real time. This is the case demonstrated to be the most critical.

Secondly, the test data set was identified. Considering that real data available at 0.28 AU are very limited and that Solar Wind models have yet to be assessed (this is one of the aims of the mission), defining relevant data sets was not a straightforward task. Acquisition conditions are very variable and CR figures are demonstrated to be very sensitive to solar wind parameters, mainly to particles density and to solar wind velocity.

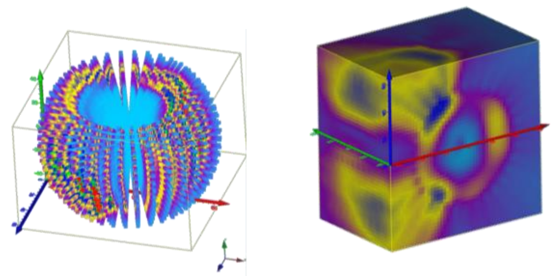

a) b)

Fig. 1. Example of a simulated 3D electrons data distribution in sensor's elevation-azimuth geometry (a) and as an acquired data cube (b).

Data acquired by the PEACE instrument (Plasma Electron And Current Experiment **Error! Reference source not found.**) onboard the Cluster mission, made similar measurements @1 AU, have been re-conditioned in order to adapt them to different acquisition conditions of EAS in the inner heliosphere. Thus, the main change is related to the Sun distance (from 1.0 to 0.28 AU). The list of the available datasets which produced results presented within this analysis is reported in the following Table 2. They have been selected in order to cover a wide range among the possible acquisition conditions the EAS sensor is expected to face in operations; a new assessment on test datasets is now on-going on this set according also to data collected from the Helios mission @0.5 AU.

Table 2. Electrons Simulated Datasets

Dataset #id	Particles Density [ppcm3]	Wind Velocity [Km/s]
DS#20080308	~3,0	~450
DS#20040302	***~2,5***	***~700-900***
DS#20070324	~2,5	~400
DS#20080406	~1,0	~700
DS#20080508	~1,0	~550
DS#20080313	~0,8	~600

Analyses on the functional compression performances have been carried out on an extended range of algorithms, considering solutions specifically designed for the space domain (CCSDS 121 [13]-[14], 122 [15] and 123 [16]) and more general ones (as lzma [17] and JPEG2000 [18]), and based on a wide set of possible compression approaches: wavelet based, dictionary based, sorting and prediction. Tests have been performed considering «off-the-shelf» software implementations (tools and libraries); a summary of the results is reported in the following Table 3.

Table 3. Compression algorithms performances trade-offs

Algorithm	***Compression Ratio (CR)***
JPEG-2000 (Mathworks Matlab)	2.26
LZMA (7-zip.org)	2.85
SZIP (© M.Schindler**)**	3.13
Rice (Basic Compression Library)	2.71
CCSDS-121 (HDF-group**)**	2.82
CCSDS-121 (ESA WhiteDwarf)	3.21
CCSDS-121 (Custom implementation)	3.23
CCSDS-122 (ESA WhiteDwarf)	2.22
CCSDS-123,SA-Modeoption (ESA)	4.09
CCSDS-123,BA-Modeoption (ESA)	4.27

The one demonstrating the best compression performance was CCSDS 123, due to the intrinsic "hyperspectral nature" of the electrons/protons VDFs.

The DPU however is equipped with a LEON2 [19] processor (running at 100 MHz), which must also remain in charge of the whole suite management (four sensors commanding, housekeeping, S/C communications, faults detection isolation and recovery), so computational resources available to compression tasks are limited.

Thus, the computational load required by CCSDS 123 is not actually sustainable via software and hence drives the need for a compression scheme combining more efficient performance, both in terms of achievable ratios and computational load. Methods taken into consideration focus on possible improvements of the pre-processing scheme, trying to identify one specifically customized to SWA data, which might provide a solution which is simpler than CCSDS-123 but still more effective than CCSDS-121.

This led to the definition of an additional data-driven mechanism based on analysis over the data and their structure has been performed: their 3D organization was investigated to evaluate compression performance on data sequences re-arranged wrt the sensor's acquisition order. Results show how a "simple" re-ordering scheme is able to improve the compression ratios by approx. 10%. The performances are strictly related to the prediction scheme: the CCSDS 121's Unit Delay predictor actually provides differences to the encoder and thus largely benefits of similarity (a slower variation rate) between next adjacent samples. However, Simple reordering schemes still entail periodical jumps in samples' order each time sensor steers back from the last to the first elevation angle or energy level.

Data can be re-ordered instead in such a way that jumps are avoided completely, always considering a sample that in the 3D space is next to the previous one, varying only one of the three indices per time. This, let's say "complex", re-ordering scheme provides a total improvement equal to up to 17.5% if compared to the custom predictor stand-alone performances, and so is able to bring the CRs to the required figure with most datasets (and the two remaining exceptions can be compensated in an overall average reasoning). The improvement becomes evident when comparing the distributions of residuals (differences between samples and their prediction); pre-processing and specifically mapping (i.e. the second step in pre-processing) are designed to fit on Laplacian distributions and they perform better as the actual residual distribution comes closer to the ideal one.

The method does not affect computational load, in terms of mathematical operations, while the possible increased amount of memory accesses has to be compensated for, including data re-ordering in data acquisition low-level logic.

3. Instrument operations perspective

All those data volume reduction strategies presented above actually depicted a broad, and worst-case, framework in which the need of a higher-level adaptive and autonomous controller of the scientific data downstream became not only sufficient but also necessary.

3.1 SWA Book-Keeping Algorithm (BKA)

Mode selection controls the "raw" telemetry rates defining time resolutions, on-board processing and data compression, i.e. the specific data products. The duty cycle among modes is designed to comply with SWA suite telemetry budget limit, assuming the expected compression ratio for each of the products can be achieved. In principle, the sensors will generate data at a rate that is significantly higher than their orbit-averaged allocation during burst modes, while normal mode data products uses somewhat less than the orbit allocation for each sensor. Thus, BKA is in essence a means to monitor and control the amount of burst mode used against the pro-rata expectation for any given point along the orbit.

Full details of the BKA are set out in project technical note [21], Owen et al. However, the principles underpinning its operation, and thus setting SWA as an intelligent decision-making system, are:

i. The BKA will be used by the DPU to assess the rate of generation of science data by each of the three SWA sensors over an established time interval that starts at time T_0 and ends at time $T_0+\Delta T$. ΔT is variable to allow for lessons learnt in flight, and the requirements imposed by variable telemetry corridors defined by the ESA SOC, but the initial baseline assumed here for illustration will be the orbital period of the S/C;

ii. The DPU will hold record of 2 limits per sensor, set by the SWA team (changeable in flight to account for lessons learnt and telemetry corridors) representing:
   a. the fractional level against which the sensors may be allowed to become overdrawn against the pro-rata allocation, and
   b. the fractional level against which an unacceptable 'underdrawing' against the pro-rata allocation is deemed to have occurred;

iii. At regular intervals the DPU will update the accumulated total volume of post-processed data which has been originated by sensor *S* since time T_0 in Burst Mode (BM)

iv. At regular intervals, the DPU will calculate the expected pro-rata data accumulation for each sensor, *S*, since time T_0, based on the orbit-averaged allocation for that sensor

v. The DPU will ensure that each sensor, *S*, does not produce so much BM data that the difference between the actual accumulated total volume of data from sensor S which has been sent to the s/c memory since time T_0 and the pro-rata orbit allocation does not exceed the fraction O_S of the remaining allocation. If the fraction is exceeded the DPU will disable optional scheduled BM and trigger event capture;

vi. In a similar way the DPU will ensure to enable additional scheduled BM

vii. In any case, the assessment period would be restarted once the period ΔT has elapsed. At this time, the accumulated data would be close to the maximum allowed total for the orbit, with only a relatively small under-/over-run.

   Thus the assessment can be restarted by carrying over the small under-/over-run to the next assessment period

The BKA is also be able to handle ground commands of the DPU operation, which set the trigger-enable flag and/or control the amount of scheduled burst mode for limited specific periods, and automatically recover the required average telemetry rate in the following period. All the parameters controlling the operation of the BKA are configurable in flight to allow the DPU to control the data production when the available telemetry rate is reduced below the nominal level.

The requirement to steer the SWA data accumulation through a defined Telemetry Corridor is equivalent to choosing a particular setting of the BKA configuration parameters defined above. This will allow the SWA BKA to control SWA telemetry generation to remain within a defined Telemetry Corridor.

3.2 Operations Telemetry Corridor(s) (OTC)

The OTC [20] is an input to instrument planning at medium-/short-term planning cycles. It is a type of resource profile for planning since it indicates to the instrument teams the allowable rates, as a function of the mission timeline, at which they can send science data to the spacecraft's SSMM via SpaceWire.

The TM volume constraints are not linked to the instantaneous data rate, but are rather about rates integrated over time. Therefore the corridors show the allowed cumulative data generation over a planning period, represented as a maximum and minimum curve. Figure 1 shows a picture representing what OTC product is.

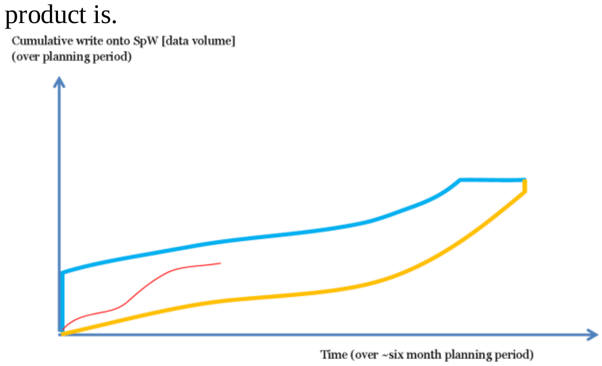

Fig. 2. Telemetry corridor simple representation [20] Image Credits: ESA]

The planning constraint element is shown with thick lines (Blue for Max, Orange for Min). The red thin line represents the measurement element, the planning period being about one-third executed in this picture. It can be seen that this illustrative instrument is operating correctly inside its constraint.

From SWA's point of view, the OTC's are intended to be defined in order to allow the ESA operations team to more finely tune the rate of telemetry generation by the instruments than the simple previous baseline, which for SWA was the generation of telemetry at a rate of 14.5 kbps averaged over a full orbit.

The BKA scheme described above, originally intended to ensure SWA meets that baseline requirement, can be practically implemented to meet the requirements of any given Telemetry Corridor.

4. Results

In order to comply with both TM allocation limits and science objectives, the approach finally defined for data compression, according to the results of tests and analyses performed, foresees a CCSDS 121 scheme, to be applied on a custom pre-processing which exploits a “complex” data-reordering scheme. The overall results with the proposed scheme, Fig. 3, if compared on the standard CCSDS 121 pre-processing, demonstrated an improvement in CR from 3,30 to 3.88, equal to 17.5% in the worst case. Figures have been evaluated as an average on 891 EAS simulated acquisitions at the worst-case solar wind’s conditions, considering the best representative compression product.

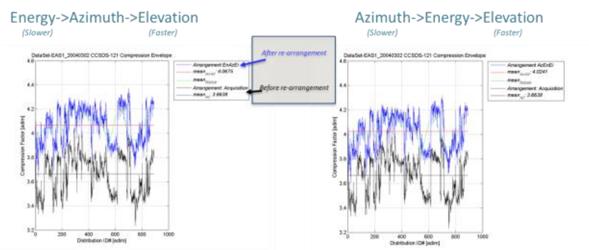

Fig. 3. CCSDS 121 CR increased performances obtained before (black line) and after (blue line) applying for two different «complex» re-ordering schema

It has to be remarked as well how for six, out of the eight data sets considered, the scheme has been able to provide a CR at least equal to the required 4.3.

This result allows us anyway to adopt the proposed approach, because the worst solar wind’s conditions will affect only a limited percentage of data acquisitions and the two exceptions are then compensated for during average acquisition cycle. Finally, the customized compression scheme, designed against electrons data particles counts, and still valid for protons, is able to meet the goal.

Nevertheless, results from simulations of the action of the BKA, defined here for the EAS sensor, which is the most challenging and critical in terms of CR figures, are shown in Figures 4 - 6.

For this sensor, the allowed total Burst mode data accumulation for the orbit (assumed here to be ΔT ~ 168 days) is ~14.4 Gbytes.

The figures show results from three examples, representing the simulated data accumulation when the average trigger mode occurrence rate is 0.1, 1.0 and 10.0 triggers per day.

For these simple examples, it is assumed that the sensor returns normal mode data (moments and 100 sec three-dimensional VDFs at the nominal rate, i.e. that the compression ratio for the latter data product remains steady at the average value of 4.3 baselined in the telemetry allocation Table 1 throughout the orbit).

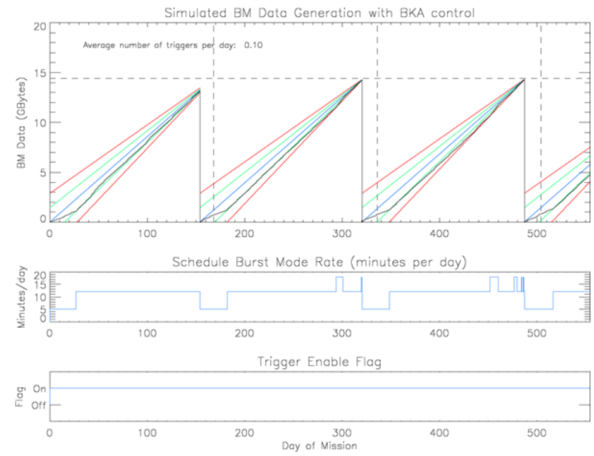

Fig. 4. Simulation of SWA/EAS data accumulation over 3.3 orbits, assuming an average trigger response rate of 0.1 per day

Considering Fig. 4, the top panel shows the simulated accumulated data rate for the scheduled burst and trigger-captured data (black trace) against the pro-rata orbit average (blue trace), the maximum and minimum acceptable data rates allowed by the BKA (2 red lines, set by parameters O_S and M described above) and the ‘re-enable levels’ (green lines, set by the fraction M also described above).

The vertical dashed lines indicate the periods of ΔT ~ 168 days used in the simulation.

The lower two panels show the number of minutes of scheduled Burst Mode allowed by the DPU and whether the response to the trigger signal is enabled or not.

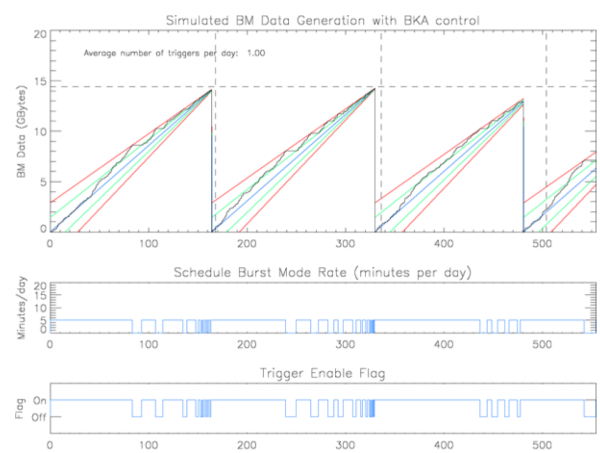

Fig. 5. Simulation of SWA/EAS data accumulation over 3.3 orbits, assuming an average trigger response rate of 1.0 per day

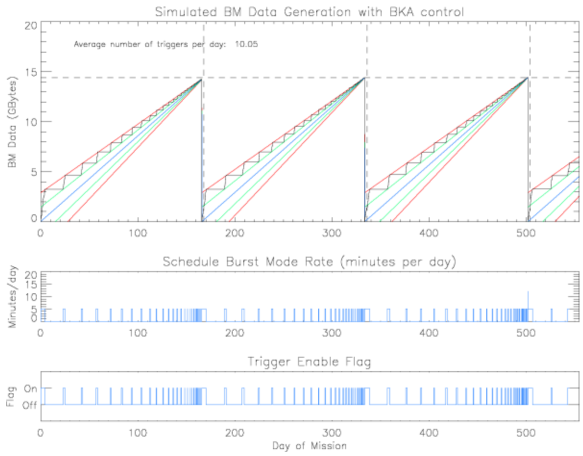

Fig. 6. Simulation of SWA/EAS data accumulation over 3.3 orbits, assuming an average trigger response rate of 10.0 per day.

5. Discussion

The increased level of autonomous scientific data assessment presents a possible solution to classical issues like bandwidth limitations, which can be conflated into the problem of data modeling. It is worth noting that onboard science data analysis will improve the capabilities of existing sensors and enable transformative new operational modes to address novel science issues thus relieving constraints on time, bandwidth and power, and by responding automatically to events on short time scales. Thus, creating unprecedented opportunities to downstream data from Space to Earth.

6. Conclusions

The technologies and methods designed for the SWA's on-board science data processing chain, are in line with the ESA OBPDP roadmap [22], see next Figure 7.

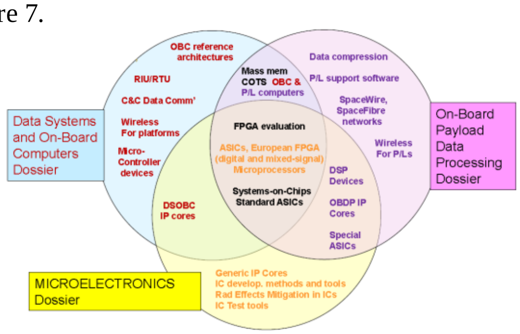

Fig. 7. ESA OBPDP roadmap [22]. Image Credits: ESA

In particular, the *Event-Driven Responsiveness* implemented by the combined adaptive compression method and the BKA, perfectly match the prioritization areas defined as AIM-A (DSP Device and Processing Modules), AIM-C (Solid State Mass Memory Modules), AIM-E (Data Compression and Processing Techniques and Systems), AIM-F (Reconfigurable Processing Modules) and AIM-G (Payload Support Software).

SWA unveils the potential for future Space missions to use onboard decision-making to detect, analyze, and respond to science events, and to downlink only the highest value science data.

Acknowledgements

We thank the whole DPU's industrial team participating in the development of the "heart" of the SWA suite, composed of TSD, Leonardo and SITAEL for both the coordination effort between the scientific team and the engineering team, especially in the frame of on-board algorithms design. Great contribution in the definition of this iterative work goes to the single sensors teams, from EAS, PAS and HIS to the entire SWA Ops Team.

References

[1] C.J. Owen et al., *The Solar Wind Analyser (SWA) Suite for Solar Orbiter*, to be submitted to A&A, October 2018
[2] European Space Agency, Definition Study Report, July 2011, "*Solar Orbiter – Exploring the Sun-heliosphere connection*"
[3] HELIOS Data Archive, http://helios-data.ssl.berkeley.edu/
[4] Rosenbauer, H., et al. (1977), *A survey on initial results of the HELIOS plasma experiment*, J. Geophys. Zeitschr. fu¨r Geophys., 42, 561 – 580.
[5] Schwenn, R., H. Rosenbauer, and H. Miggenrieder (1975), *Das Plasmaexperiment auf Helios*, Raumfahrtforschung, 19, 226.
[6] CLUSTER SCIENCE DATA SYSTEM (CSDS), http://sci.esa.int/cluster/52770-csds/
[7] Escoubet, C., R. Schmidt, and M. Goldstein (1997), Cluster: *Science and mission overview*, Space Sci. Rev., 79, 11– 32
[8] Johnstone, A. D., Alsop, C., Burge, S., Carter, P. J., Coates, A. J., Coker, A. J., Fazakerley, A. N., Grande, M., Gowen, R. A., Gurgiolo, C., Hancock, B. K., Narheim, B., Preece, A., Sheather, P. H., Winningham, J. D., and Woodliffe, R. D.: *Peace: A plasma electron and current experiment*, Space Science Reviews, 79, 351-398, doi:10.1023/a:1004938001388, 1997
[9] Acuña, M. H., K. W. Ogilvie, D. N. Baker, S. A. Curtis, D. H. Faireld, and W. H. Mish (1995), The Global Geospace Science Program and Its Investigations, Space Sci. Rev., 71, 5{21, 10.1007/BF00751323
[10] Garrard, T.~L., Christian, E.~R., Mewaldt, R.~A., Ormes, J.~F., Stone, E.~C., 1997, *The Advanced Composition Explorer Mission*, International Cosmic Ray Conference 1, 105
[11] Gowan and Birdseye, March 1988, *Extracting Bulk Parameters of a Particle Distribution*

[12] E. Marsch, K.-H. Muhlhauser, R. Schwenn, H. Rosenbauer, W. Pilipp, F.M. Neubauer, JGR, 87,1982 *Solar Wind protons: Three-dimensional velocity distributions and derived plasma parameters measured between 0.3 and 1 AU*
[13] Rice R., *Some Practical Universal Noiseless Coding Techniques-Part III.* Module PSI14.K, Jet Propulsion Laboratory, JPL Publication 91-3, Pasadena, CA, 1991
[14] ESA, Data Compression Tools, *WhiteDwarf data compression evaluation tool*, http://www.esa.int/TEC/OBDP/SEM069KOXDG_2.html
[15] University of Nebraska Lincoln, Department of Electrical Engineering, *An implementation of CCSDS 122.0-B-1 Recommended Standard* http://hyperspectral.unl.edu/
[16] ESA, Data Compression Tools, *An implementation of the new CCSDS 123 Recommended Standard*, http://www.esa.int/TEC/OBDP/SEM069KOXDG_0.html
[17] Basic Compression Library, *A set of open source implementations of several lossless compression algorithms* (Huffman, RLE, Rice, Lempel-Ziv-77 and Shannon-Fano), http://www.bcl.comli.eu
[18] ISO/IEC 15444-1:2004, *JPEG 2000 Image Coding System: Core Coding System*, 2nd ed., 2004
[19] 7703E–AERO–08/11, *AT697F Rad-Hard 32 bit SPARC V8 Processor*
[20] C. Watson, March 2017, *Solar Orbiter TeleMetry Corridor ICD*, European Space Agency
[21] Owen et al., *Solar Orbiter SWA Scientific Operations, Algorithms and Processes Requirements Document*, SO-SWA-MSSL-RQ-010
[22] M. Suess, R. Trautner, R. Vitulli, D. Thurnes, D. Jameux, J. Both, *TECHNICAL DOSSIER ON ON-BOARD PAYLOAD DATA PROCESSING*, ESA/IPC/THAG(2016)xx Issue 4 rev 0 02/10/2015